

Metaecosystem Dynamics of Marine Phytoplankton Alters Resource Use Efficiency along Stoichiometric Gradients

Nils Gülzow,¹ Yanis Wahlen,¹ and Helmut Hillebrand^{1,2,*}

1. Institute for Chemistry and Biology of the Marine Environment, Carl von Ossietzky University of Oldenburg, Schleusenstrasse 1, 26382 Wilhelmshaven, Germany; 2. Helmholtz Institute for Functional Marine Biodiversity at the University of Oldenburg, Ammerländer Heerstrasse 231, 26129 Oldenburg, Germany

Submitted April 3, 2018; Accepted August 21, 2018; Electronically published November 27, 2018

Online enhancements: appendixes. Dryad data: <https://dx.doi.org/10.5061/dryad.km10jq1>.

ABSTRACT: Metaecosystem theory addresses the link between local (within habitats) and regional (between habitats) dynamics by simultaneously analyzing spatial community ecology and abiotic matter flow. Here we experimentally address how spatial resource gradients and connectivity affect resource use efficiency (RUE) and stoichiometry in marine phytoplankton as well as the community composition at local and regional scales. We created gradostat metaecosystems consisting of five linearly interconnected patches, which were arranged either in countercurrent gradients of nitrogen (N) and phosphorus (P) supply or with a uniform spatial distribution of nutrients and which had either low or high connectivity. Gradient metaecosystems were characterized by higher remaining N and P concentrations (and N:P ratios) than uniform ones, a difference reduced by higher connectivity. The position of the patch in the gradient strongly constrained elemental stoichiometry, local biovolume production, and RUE. As expected, algal carbon (C):N, biovolume, and N-specific RUE decreased toward the N-rich end of the gradient metaecosystem, whereas the opposite was observed for most of the gradient for C:P, N:P, and P-specific RUE. However, at highest N:P supply, unexpectedly low C:P, N:P, and P-specific RUE values were found, indicating that the low availability of P inhibited efficient use of N and biovolume production. Consequently, gradient metaecosystems had lower overall biovolume at the regional scale. Whereas treatment effects on local richness were weak, gradients were characterized by higher dissimilarity in species composition. Thus, the stoichiometry of resource supply and spatial connectivity between patches appeared as decisive elements constraining phytoplankton composition and functioning in metaecosystems.

Keywords: biodiversity, dispersal, metacommunity, ecological stoichiometry, nutrient gradient.

Introduction

Ecological communities are open to dispersal, allowing for immigration of organisms into local habitats (patches), which are regionally connected (Elton 1958). Major frameworks have emerged from the need to understand how local interactions within patches and regional processes between patches interact in controlling community composition and functioning in spatially structured environments, for example, landscape ecology (Turner 1989, 2005) and metacommunity theory (Leibold and Mikkelsen 2002; Leibold et al. 2004; Holyoak et al. 2005). Integrating aspects of both approaches, Loreau et al. (2003b) and Loreau and Holt (2004) coined the term “metaecosystem” to describe a region with multiple habitat patches, which are linked by exchange of organisms and the simultaneous flow of matter and energy.

This integrated assessment of biotic and abiotic spatial dynamics has led to major theoretical advances in recent years (Massol et al. 2011; Gounand et al. 2018). Metaecosystem models analyzed the effects of combined and separate spatial movement of food web compartments (nutrient[s], primary producer, herbivore, and detritus) and thereby offered new insights on source-sink dynamics (Gravel et al. 2010a), the consequences of resource enrichment (Gounand et al. 2014), species coexistence (Gravel et al. 2010b), and consequences of perturbations (Harvey et al. 2016). Beyond these studies, metaecosystem approaches are also at the core of new approaches to understand biodiversity and ecosystem functioning based on community assembly processes (Haegeman and Loreau 2014; Leibold et al. 2017) and spatial subsidies across ecosystems based on resource flow and dispersal (Leroux and Loreau 2012; Soininen et al. 2015; Gounand et al. 2017, 2018).

Resource stoichiometry can play a central role in metaecosystem (and metacommunity) ecology given that inequalities in resource availability play a central role in diffusive matter fluxes as well as spatial patterns of coexistence and resource use. Unequal distribution of resources across patches has been incorporated in both metacommunity and meta-

* Corresponding author; email: helmut.hillebrand@uni-oldenburg.de.

ORCID: Hillebrand, <http://orcid.org/0000-0001-7449-1613>.

Am. Nat. 2019. Vol. 193, pp. 35–50. © 2018 by The University of Chicago. 0003-0147/2019/19301-58377\$15.00. All rights reserved.

DOI: 10.1086/700835

ecosystem theory. In a metacommunity model allowing for organism dispersal (but no inorganic matter flow) between adjacent patches, Hodapp et al. (2016) simulated the effect of two aspects of stoichiometric heterogeneity: (i) the same regional amount of two nutrients distributed with increasing spatial heterogeneity across space, increasing the stoichiometric difference in resource supply between patches and the imbalance within patches, and (ii) the differences in resource needs between species, with increasing trait variance reflected by increasing difference in optimal ratios between species. In this model, higher spatial variance in resource supply ratios led to lower total biomass production, as stoichiometric imbalance prevented the complete use of both resources. However, with increasing trait variance, local and regional coexistence increased in stoichiometrically more divergent metacommunities and through strong complementarity effects led to higher resource use efficiencies (RUEs) in mixtures than expected from single species. These simulations corroborated conclusions from a much simpler but analytically tractable model comprising only two species (Gross and Cardinale 2007). They showed that if species can coexist on countercurrent resource gradients, then this coexistence leads to more efficient transformation of available resources into biomass production.

In a metaecosystem context, these stoichiometric considerations have to be extended to include diffusion of nutrients between patches, where imbalanced supply triggers inorganic matter flow from patches with high concentrations to patches with low concentrations. Marleau et al. (2015) included nonmobile plants with mobile herbivores (movement) and nutrients (diffusion) in their model to test for the occurrence of colimitation by multiple resources. They concluded that colimitation, which is often detected in fertilization experiments (Harpole et al. 2011), can occur through spatial nutrient flows even if the stoichiometry of local resource supply ratios would indicate limitation by single resources. Extending this approach to stoichiometric distribution models, Leroux et al. (2017) linked this stoichiometric metaecosystem approach to macroecology: parametrized for a spatial herbivore/plant (moose/birch) case, they were able to predict consumer space use based on a spatial assessment of the elemental composition of their resources.

As for metacommunity ecology (Logue et al. 2011), the theoretical advancement on metaecosystems has been much faster than the development of empirical assessments. Few metaecosystem experiments have been performed at the microcosm scale (Harvey et al. 2016; Gounand et al. 2017) and the mesocosm scale (Legrand et al. 2012; Limberger et al. 2017). Most of these experiments focused on differentiating between the mobility of abiotic resources and organisms, whereas experiments manipulating spatial resource stoichiometry are largely missing. Given that spatial heterogeneity

in resource supply is supposed to alter the coexistence of species (metacommunity dynamics) and abiotic resource flow (metaecosystem dynamics), we need empirical information on the interplay of both aspects and its interrelation to connectivity.

An elegant way to address these questions is using gradostat experiments that arrange patches in the form of a chain and thus represent linear metaecosystems allowing for organism dispersal and matter flow. Codeco and Grover (2001) used gradostats to test how countercurrent gradients of resources alter coexistence and performance of communities in comparison to spatially homogeneous resource arrangements. They found increased local diversity with the gradient compared to without it, because locally inferior species could be maintained by source-sink dynamics from neighboring positions in the gradostat.

Adopting the gradostat idea, we connected five Erlenmeyer flasks (patches) to their neighbors by silicone tubes to form linear metaecosystems. We inoculated all patches with a multispecies assemblage of marine phytoplankton and manipulated the connectivity between patches (high and low dispersal; for details, see “Methods”) and the spatial supply of two limiting resources, nitrogen (N) and phosphorus (P). For the latter, we supplied identical N and P concentrations to all serially arranged patches (molar N:P ratio = 15; “uniform”) or we supplied the full amount of P to one final patch of the series and all N to the opposite end of the metaecosystem (“gradient”). Whereas all treatment combinations were manipulated in a full-factorial design, they are intentionally not entirely independent: in higher-connectivity metaecosystems, the gradient in nutrient supply ratios will be homogenized more than under low connectivity. This design allowed us to test the following hypotheses:

H1: Gradient metaecosystems are characterized by lower efficiency of resource incorporation than uniform ones (H1a), as less of the available N and P is incorporated if supplied at imbalanced ratios (cf. Gross and Cardinale 2007; Hodapp et al. 2016). As algal stoichiometry is often linked to the stoichiometry of nutrient supply, we further expect a significant effect of patch position on algal nutrient ratios in the gradient (but not in the uniform) metaecosystems (H1b). This association between supply and incorporation can be linear (from low N:P and C:P at the P-rich end of the gradient to low C:N and high N:P at the N-rich end) or unimodal, if highly imbalanced supply ratios at both ends of the gradient impair incorporation of the replete nutrient. Finally, we expect that the differences between gradient and uniform supply treatments will be reduced with increasing connectivity, as this allows exchange of matter via abiotic flows and thus

a reduction in the strength of the nutrient gradient (H1c).

- H2: Based on existing models (Gross and Cardinale 2007; Hodapp et al. 2016), we predict a lower RUE (biomass produced per available resource) at imbalanced supply ratios. Therefore, gradient metaecosystems are characterized by lower biovolume (equivalent to biomass) production at the regional level than uniform metaecosystems and—especially at low connectivity—a decrease of local RUE toward both ends of the gradients with the most imbalanced supply ratios.
- H3: Based on the abovementioned studies (Codeco and Grover 2001; Hodapp et al. 2016), we expect more species coexisting in the gradient than in the uniform metaecosystem, as well as a higher dissimilarity in species composition between patches. The effect of connectivity on biodiversity can be positive or negative, depending on the nonlinear effect that dispersal can have on local coexistence (Loreau et al. 2003a).

Methods

Cultivation and Experiment Preparation

All phytoplankton taxa used in the experiment were isolated from the North Sea and comprised five diatom species (*Thalassiosira hendeyi* Hasle & Fryxell; *Ceratoneis closterium* Ehrenberg; *Mediopyxis helysia* Kühn, Hargreaves & Halliger; *Stephanopyxis turris* (Greville) Ralfs; and *Gyrosigma* sp.) and one cryptophyte species (*Teleaulax* sp.). Species will be identified by their genus names for the remainder of the article. All stock cultures were kept in an 18°C temperate climate chamber under a light intensity of 80 $\mu\text{E m}^{-2} \text{s}^{-1}$ and a 12L:12D photocycle. Stock cultures were cultivated in a 250 mL culture flask with 0.2 μm of enriched filtered seawater ($f/2$; 883 $\mu\text{mol L}^{-1}$ NaNO_3 , 36.3 $\mu\text{mol L}^{-1}$ NaH_2PO_4 , and 107 $\mu\text{mol L}^{-1}$ Na_2SiO_3) according to Guillard and Ryther (1962). Average cellular biovolume (μm^3) of each species was estimated by measuring 20 randomly chosen individuals with an inverted microscope (DM IL LED; Leica) following Hillebrand et al. (1999) and—for *Gyrosigma*—Olenina et al. (2006). Prior to the experiment, initial cell concentration (cell mL^{-1}) and the species-specific biovolume concentration ($\mu\text{m}^3 \text{mL}^{-1}$) were estimated for each species to equalize inoculated biovolume at the onset of the experiment.

The 0.2 μm of filtered seawater required for the experiment was prepared in one batch and stored in the dark at

4°C until used. We added all nutrients except N and P according to $f/2$ concentrations (Guillard and Ryther 1962). We created four different media with the following concentrations of N and P, based on the background concentrations in the filtered seawater and enrichment reflecting $f/2$ concentrations: (i) fully enriched seawater medium (347 $\mu\text{mol L}^{-1}$ NaNO_3 , 30.6 $\mu\text{mol L}^{-1}$ NaH_2PO_4 , and 80 $\mu\text{mol L}^{-1}$ Na_2SiO_3), (ii) nitrogen-limited ($-N$) medium (85.4 $\mu\text{mol L}^{-1}$ NaNO_3 , 31.3 $\mu\text{mol L}^{-1}$ NaH_2PO_4 , and 95 $\mu\text{mol L}^{-1}$ Na_2SiO_3), (iii) phosphorus-limited ($-P$) medium (355 $\mu\text{mol L}^{-1}$ NaNO_3 , 4.5 $\mu\text{mol L}^{-1}$ NaH_2PO_4 , and 87 $\mu\text{mol L}^{-1}$ Na_2SiO_3), and (iv) both $-N$ and $-P$ medium (47.9 $\mu\text{mol L}^{-1}$ NaNO_3 , 1.6 $\mu\text{mol L}^{-1}$ NaH_2PO_4 , and 88 $\mu\text{mol L}^{-1}$ Na_2SiO_3). Media with limitation by either N, P, or both contained only the background N and P concentrations present in the seawater at filtration, which are typical for in situ concentrations from the same coastal region before spring bloom (80 $\mu\text{mol L}^{-1}$ N and 0.5 $\mu\text{mol L}^{-1}$ P; Grunwald et al. 2007). N and P were added if they were supposed to be nonlimiting at concentrations allowing algal growth and biovolume buildup during the experiment. The deviations in the actual concentrations reflect slight discrepancies in the background concentrations of the filtered seawater.

Experimental Setup and Sampling. The experiment compared the connectivity (low vs. high) and spatial resource supply (uniform vs. gradient) in metaecosystems consisting of five linearly arranged and connected patches (app. A; apps. A–D are available online). All combinations of connectivity and spatial resource treatments were replicated threefold at the metaecosystem level (i.e., independent $2 \times 2 \times 3 = 12$ metacommunities, consisting of 60 local patches in total). Each patch consisted of a 50 mL Erlenmeyer flask that was serially connected by silicone tubes (7 cm length, 5 mm diameter) to the neighboring flasks, such that intermediate flasks were connected to two patches and the final flasks to one other patch.

The experimental setup was mounted on a horizontal shaker (60 rpm) to keep algae in suspension and to induce small-scale water movement between patches. Clamps on the tubes allowed for different connectivity treatment. At low connectivity, tubes were opened for 10 min every second day, whereas at high connectivity, tubes were opened for 1 h per day. When opened, water movement, diffusion, and active movement of organisms allowed for matter flow and dispersal between patches. To estimate lateral nutrient flows between patches (app. A), we performed an extra experiment without organisms (app. B). This experiment showed the change in the nutrient gradient with increasing opening time of the silicone tube, which reflects the net exchange of nutrients between neighboring flasks based on abiotic matter exchange. Using this information as well as the initial and replenishment supply of nutrients, we were

able to quantify the amount of N and P available at each patch position (see below) but without lateral transfer by organisms (app. B). Half of the inoculated species demonstrated active movement by crawling on a polysaccharide layer (*Gyrosigma* and *Ceratoneis*) or by using a flagella (*Teleaulax*), whereas the other species were transported only by turbulent motion of the medium (*Thalassiosira*, *Mediopyxis*, and *Stephanopyxis*). Therefore, the selected species comprise a broad range in active movement and thus colonization ability.

The experiment was conducted in a climate chamber at 18°C with a light intensity of 80 $\mu\text{E m}^{-2} \text{s}^{-1}$ and a 12L:12D photocycle. Each metaecosystem was supplied with roughly the same total amount of N and P (uniform: 107.7 $\mu\text{mol L}^{-1}$ N and 7.3 $\mu\text{mol L}^{-1}$ P; gradient: 116.8 $\mu\text{mol L}^{-1}$ N and 8.1 $\mu\text{mol L}^{-1}$ P), with the small differences reflecting slightly different background nutrient concentrations in the filtered seawater. For the gradient treatment, only patch 1 received added N (medium iii), whereas only patch 5 received added P (medium ii). Patches 2–4 received the $-N/-P$ medium (iv) and thus only the background concentrations present in the natural seawater. In the uniform treatment, N and P amounts were equally partitioned among all five patches using a mixture of media i and iv.

Each flask (patch) was inoculated with all six species, each contributing equal proportions to the initial biovolume of 185,800 $\mu\text{m}^3 \text{mL}^{-1}$. During a period of 4 weeks, the experiment was sampled weekly (day 7, 14, 21, 28). Each sample removed 20% of the entire volume, which was immediately replaced by an equal amount of fresh medium with the exact corresponding nutrient concentrations as in the starting conditions for the respective patch position. Thus, sampling and replacement resulted in a semicontinuous culturing regime with a weekly exchange of 20%, which corresponds to a dilution rate of 0.03 per day.

Samples for counting (10 mL) were fixed with 1% Lugol's solution in brown glass bottles. An aliquot of 1 mL was used to determine the species composition and biovolume using Utermöhl counting chambers and an inverted microscope. Depending on cell size (<10 μm or >10 μm diameter), different magnifications were used ($\times 40$ and $\times 100$, respectively). For each species, at least 400 cells (or at very low abundance, the entire counting chamber) were counted. Count data were transferred to algal biovolume by multiplying abundance with the cell volume as described above. At the end of the experiment, we checked cell sizes microscopically again for each species and in each treatment. We found no obvious deviation from the cell sizes calculated at the start.

Biodiversity at both local (patch) and regional (metaecosystem) scales was assessed using the effective number of species (ENS), which has been described as a robust measure of diversity (Chase and Knight 2013). ENS is based on the inverse Simpson index and was calculated using

biovolume proportions. To calculate dissimilarity between patches in a metaecosystem, we used the Bray-Curtis dissimilarity (Bray and Curtis 1957). Please note that regional ENS is not simply an average of the local ENS values but was calculated from proportions of species to total regional biovolume. ENS and Bray-Curtis dissimilarity were calculated using the *vegan* package in R (Oksanen et al. 2015).

At day 28, we destructively sampled the entire units. A volume of 10 mL (>500 μg carbon [C]) was filtered through precombusted GF/F filters (Whatman; 25 mm diameter), one for measurement of particulate C and N and one for P. The remaining filtrate was retained in scintillation vials for dissolved nutrient analysis. The CN and P filters were stored in a compartment drier at 60°C, whereas the dissolved nutrient samples were frozen at -18°C until analysis. The CN analyses were done using a CHN analyzer (FlashEA, 1112 Series; Thermo Scientific), while particulate P was analyzed photometrically as orthophosphate after heat digestion and acidic hydrolysis with 5% H_2SO_4 (modified from Grasshoff et al. 1983) using a spectrophotometer (U3000; Hitachi). Dissolved N and P were measured with a photometric autoanalyzer (San⁺⁺; Skalar).

RUE was calculated by dividing the biovolume produced ($\mu\text{m}^3 \text{mL}^{-1}$) by the supply of P (RUE_P) or N (RUE_N), both measured as $\mu\text{mol mL}^{-1}$. RUE is thus in units of μm^3 biovolume per available μmol of the respective nutrient. The available amount of the nutrient in a single patch was summed up from its initial stock at the start of the experiment, the added amount when replacing sampled volume by equivalent volume of the respective medium, and by estimating the lateral inflow from the neighboring patch with the higher concentration of this nutrient (app. B). We caution that this approach does not include potential additional spatial fluxes of N or P induced by differential nutrient uptake by the local algal community in one patch and movement of algae between patches. However, given the strong resource gradient across the patches (app. B), we are confident that exchange by water movement and diffusion are the major aspects of lateral nutrient flow, such that the estimated supplies remain realistic.

Statistical Analyses. Full data can be found in the Dryad Digital Repository: <https://dx.doi.org/10.5061/dryad.km10jq1> (Gülzow et al. 2018). All statistical tests on the hypotheses H1–H3 were performed with R version 3.4.0 (R Development Core Team 2015). As a graphical tool, we used the *ggplot2* package in R (Wickham 2009). Stoichiometric response variables were available for the end of the experiment (day 28) only, whereas biovolume, RUE, and diversity measures were measured multiple times. Therefore, we tested H1 by using the final outcome but tested H2 and H3 over time. Moreover, each test was conducted separately for regional and local variables.

For the effects of treatments on nutrient incorporation and its stoichiometry (H1), we performed these regional and local tests on remaining dissolved N and P, their molar N:P ratio, and the molar ratios of algal stoichiometry (C:N, C:P, N:P). At the regional level, a two-factorial ANOVA comprised connectivity (low, high) and spatial resource supply (uniform, gradient) as independent factors. Testing the hypotheses at the local scale required the inclusion of patch position in the analyses and the accounting for the nonindependence of the connected patches. Therefore, we performed a mixed effect model using connectivity (low, high) and spatial resource supply (uniform, gradient) as interacting orthogonal fixed factors as well as patch position (1–5) as categorical factor nested under spatial resource supply. Using the lme4 package in R (Bates et al. 2015), we used metaecosystem identity (1–12) as random factor, which created the corresponding error mean squares for each factor. The fixed factors were tested against the true degrees of freedom ($df = 1, 8$) given the 12 independent systems, except the nested patch position was tested with $df = 8, 40$. We used the lsmeans package in R version 2.27-2 to perform post hoc tests for significant difference between treatment levels (Lenth 2016). Given the experimental design, we used standard significance values for the F ratios that were found.

For H2, response variables were total biovolume as well as RUE_P and RUE_N ; for H3, response variables were ENS and Bray-Curtis dissimilarity in species composition. We performed an analysis over time using a linear mixed model with the same factors as mentioned above. Additionally, we included days as a continuous fixed factor and as a categorical random factor. We thereby distinguished between random variations among sampling points and at the same time tested for a significant temporal change reflected by the slope of the continuous sampling time variable.

We achieved homogenous variances and normal distribution for almost all tests and response variables, with the exception of the remaining dissolved nutrients at the regional scale (H1). To secure that observed treatment effects were not solely due to the remaining heteroscedasticity, we used a Kruskal-Wallis test on the four combinations of connectivity and spatial resource supply levels and found qualitatively the same results. Therefore, we provide only the ANOVA results in this article.

Results

Nutrient Incorporation in Resource Supply Gradients of Different Connectivity (Hypothesis H1)

Regionally, significantly more N and P remained dissolved (and thus unused) at the end of the experiment in the gra-

dient metaecosystem compared to the uniform ones (fig. 1a, 1b; table 1, significant main effect of spatial resource supply). This gradient effect on remaining concentrations was larger for N than for P, and for N the difference was significantly larger at low connectivity (table 1, significant interaction). Consequently, the N:P ratio of the remaining dissolved nutrients was significantly higher in the low-connectivity gradient metaecosystems than in any other treatment combination (fig. 1c; table 1).

At the local patch scale, significant effects of spatial resource supply and connectivity on remaining N and P were similar to those observed at the regional level: higher final concentrations of both nutrients in gradient metaecosystems and higher N concentrations in low-connectivity gradients (table 1). Moreover, patch positions significantly affected remaining local N and P concentrations in the gradient metaecosystems but not in the uniform ones (table 1; fig. 1e): remaining N—as well as the dissolved N:P ratio—decreased from patch 1 and 2 ($1 = 2 > 3 = 4 = 5$), and remaining P decreased from patch 5 ($5 > 4 = 3 = 2 = 1$). Consequently, the N:P ratio of remaining dissolved nutrients reflected the ratio of N:P supply in the low-connectivity gradients but was higher than the supply ratio in the N-rich patches 1 and 2 (fig. 2a). By contrast, the remaining N:P in highly connected gradients was no longer affected by supply N:P and was overall similar to the remaining N:P in uniform treatments.

The algal elemental ratios, reflecting nutrient incorporation, differed with spatial resource supply both regionally and locally. The signs of the effects on algal ratios in most cases were opposite to the treatment effects on remaining nutrients, reflecting that the proportion of the incorporated supply affected the remaining concentration. Consequently, regional algal N:P was higher in uniform than in gradient metaecosystems but only at low connectivity (fig. 1d; table 1, marginally nonsignificant interaction). Both regionally and locally, algal C:P ratios were significantly higher in uniform than in gradient metaecosystems; the same effect could be observed for C:N but with the effect being marginally nonsignificant (table 1; app. C).

The effect of patch position on local algal stoichiometry was significant for all three ratios (table 1). Algal N:P significantly increased from patch 1 to 2 and then decreased toward the P-rich positions 4 and 5 (table 1; fig. 1f). This unimodal response to patch position was significant across connectivity treatments (table 1), but plotting algal N:P to N:P supply showed that the nonlinearity was more pronounced in the low-connectivity treatment (fig. 2b). Moreover, in low-connectivity gradients algae incorporated relatively more N than supplied, that is, algal N:P was consistently higher than the supply ratio, except for the highest N:P supply patch 1. Here algal N:P was much lower than N:P supply, which coincided with high remaining N concentrations and N:P ratios

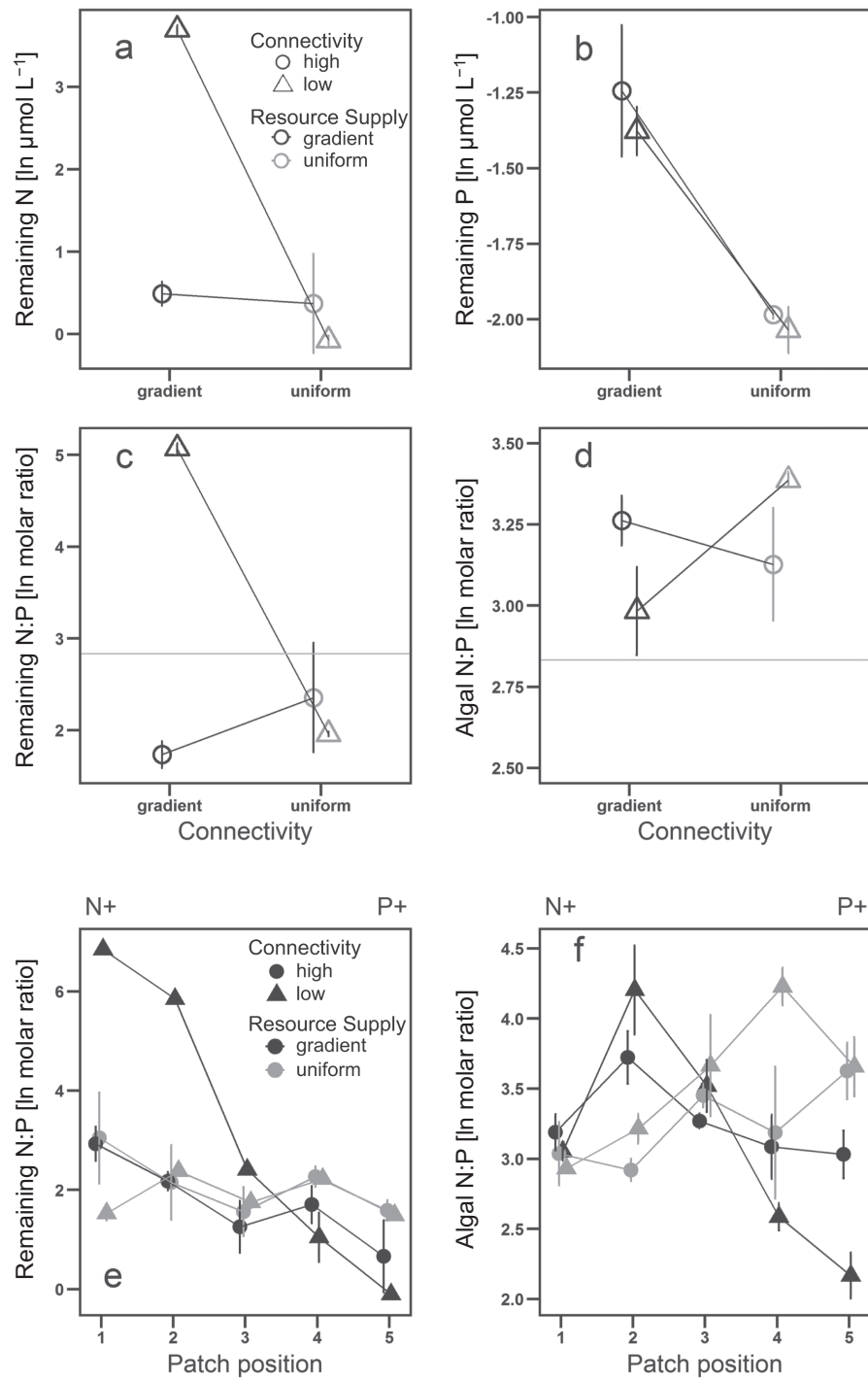


Figure 1: Effects of spatial resource supply and connectivity on the stoichiometry of nutrient incorporation and remaining dissolved nutrients at the end of the experiment (day 28) at regional (*a-d*) and local (*e, f*) scales. Error bars indicate standard error (± 1 SE). Open symbols reflect variables measured at the regional scale of the entire metaecosystem; filled symbols reflect variables measured at the local patch scale. Gray and black symbols reflect uniform and gradient metaecosystems, respectively. Symbols denote low (triangle) and high (circle) connectivity. *a, b*, Regional concentrations of dissolved nitrogen (N) and phosphorus (P). *c*, Dissolved N:P molar ratio. *d*, Algal N:P molar ratio. *e*, Local molar N:P ratio of remaining nutrients across patch position in uniform and gradient metaecosystems of high or low connectivity. *f*, Local algal molar N:P ratio across patch position in uniform and gradient metaecosystems of high or low connectivity.

Table 1: Summary of the statistical analyses for nutrient-related response variables at regional and local scales at the end of the experiment (day 28)

	N rem	P rem	N:P rem	N:P algae	C:P algae	C:N algae
Regional:						
SRS	39.06 [<.001] G > U	33.00 [<.001] G > U	16.37 [.004] G > U	1.31	7.44 [.026] G < U	5.10 [<i>.054</i>] G < U
CON	19.56 [.002] L > H	.57	22.75 [.001] L > H	.01	.50	.75
SRS × CON	34.33 [<.001] G:L > all	.11	36.71 [<.001] G:L > all	5.25 [<i>.051</i>] U:L > G:L	.05	3.75 [<i>.089</i>] U:H > G:H
Local:						
ME ID	0%	0%	<1%	0%	21.16%	27.04%
SRS	14.62 [<.001] G > U	51.89 [<.001] G > U	3.13 [<i>.083</i>] G > U	4.37 [<i>.058</i>] G < U	6.32 [.036] G < U	5.47 [<i>.051</i>] G < U
CON	4.08 [.049] L > H	.69	5.07 [.028] L > H	.3	.89	.16
SRS × CON	9.93 [<.001] U:H > all	.01	10.01 [<.001] U:H > all	3.92 [.030] U:L > U:H	<.01	3.9
Patch position SRS	6.66 [<.001] G: (1, 2) > (3, 4, 5)	8.51 [<.001] G: 1 < 4; (1, 2, 3, 4) < 5	10.37 [<.001] G: (1, 2) > (3, 4, 5)	6.88 [<.001] G: 1 < 2; 2 > (4, 5); 3 > 5	6.25 [<.001] G: 1 < (2, 3) > 5; U: 2 < (3, 4, 5)	3.2 [.028] G: 1 < (3, 4)

Note: Fixed factors comprised the treatments' spatial resource supply (SRS) and connectivity (CON) at both scales. At the local scale, patch position (nested in SRS) was added as a fixed effect and metacosystem ID (ME ID) was added as a random factor. Response variables comprised the remaining concentrations of dissolved nitrogen (N rem) and phosphorus (P rem) and their molar ratio (N:P rem) and the molar ratios of N:P, C:N, and C:P within the algae. Response variables were log transformed to achieve homogenous variances (see "Methods"). We report *F* ratios (df = 1, 8, except for the nested patch factor with df = 8, 40) as well as significance levels for all factors with *P* < .1 in brackets. We report significant differences for post hoc comparisons, abbreviating SRS levels as G (gradient) and U (uniform) and CON levels as L (low) and H (high). Boldface data indicates that *P* < .05, and italicized data indicates that .1 > *P* > .05.

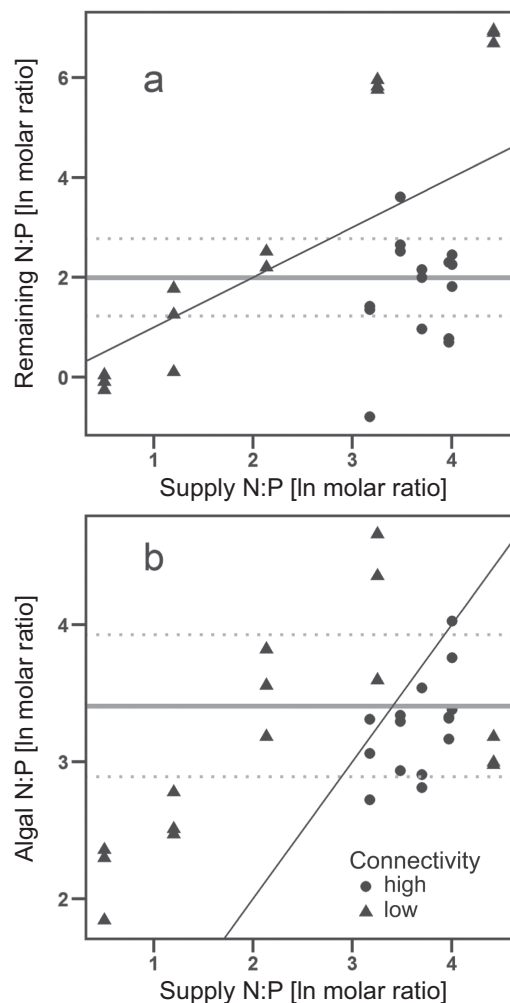


Figure 2: Local remaining (*a*) and algal (*b*) molar nitrogen:phosphorus (N:P) ratio against N:P ratio of the supplied nutrients for the gradient treatment. Symbols denote low (triangle) and high (circle) connectivity. The observed algal N:P in the uniform treatments is given for reference as mean (solid gray line) \pm standard deviation (dotted gray lines) for comparison. The solid black line is the 1:1 line between supply and incorporation.

observed in these patches (figs. 1*d*, 2*a*; table 1). In highly connected gradients, by contrast, algal N:P was lower than supplied and generally within the range observed in the uniform metaecosystems (fig. 2*b*).

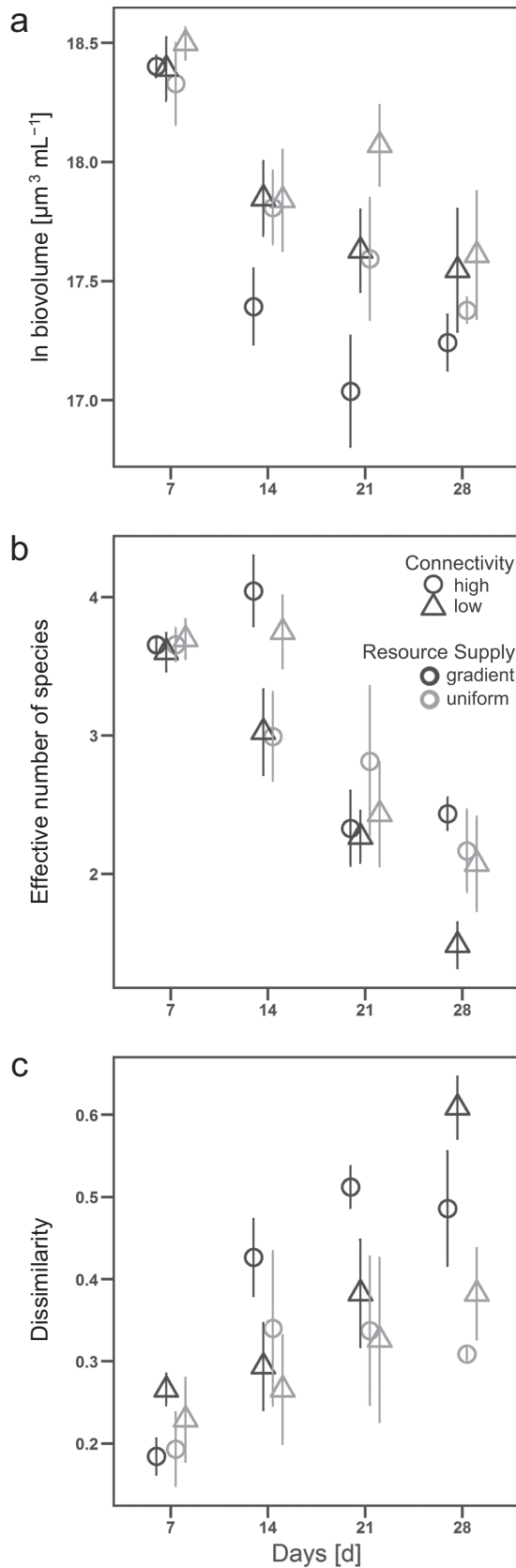
Algal C:P ratios showed very similar patterns as seen for N:P. In gradient metaecosystems, C:P was highest at patches 2 and 3 and significantly lower at patch 5 (reflecting the high P supply) and patch 1 (despite low P supply; app. C, fig. C1*a*, C1*b*). Again, the pattern was more pronounced under low connectivity. Algal C:N was less variable and generally reflected the supplied amount of N: patch 1 was characterized by significantly lower algal C:N than patches 3 and 4 (table 1; fig. C1*c*, C1*d*).

Biovolume and RUE (Hypothesis H2)

Regional biovolume increased rapidly from inoculation to the first sampling at day 7 (approximately two orders of magnitude), after which it declined over time (fig. 3*a*; table 2, significant negative main effect of time). Regional biovolume also significantly decreased with higher connectivity and was lower in gradient than in uniform metaecosystems (table 2, marginally nonsignificant effect). Also at the local scale, biovolume was significantly reduced in gradient metaecosystems as well as at high connectivity and declined over time (table 1). The significant effect of patch position and the significant interaction between time and spatial resource supply reflected that the decrease in biovolume was most pronounced at the P-poor end of the gradient (fig. 4*a*). Local biovolume was significantly higher at the P-rich end of the gradient (patch positions 3–5) compared to the opposite N-rich end (position 1; table 2) and lower than in the uniform metaecosystems.

Normalizing local biovolume production to the available supply of N (RUE_N) or P (RUE_P) reinforced these observations but revealed important temporal dynamics (fig. 4*b*, 4*c*). In the uniform metaecosystems, RUE_N only slightly decreased over time and was constant across patch position. In the gradient metaecosystems, RUE_N declined over time, especially in patches 1 and 2 at low connectivity, resulting in a steep increase from the N-rich end of the gradient to the P-rich end (fig. 4*b*). At higher connectivity, the same trend was observable but much less pronounced. Compared to the uniform metaecosystems, the phytoplankton in gradients was much less effective in transferring available N into biovolume if N was replete but was more effective if it was highly limiting. All corresponding statistical results were significant (table 2: main effects and interaction of spatial resource supply and connectivity, nested effect of patch position in gradient metaecosystems, temporal decline depending on spatial resource supply). Moreover, the pattern reflected the N:P ratio of remaining nutrients and the C:N and N:P ratios of phytoplankton biomass.

Even faster than RUE_N , RUE_P showed a linear—and countercurrent, thus negative—trend with patch position in the gradient metaecosystems (fig. 4*c*). After 2 weeks, RUE_P declined from the N-rich end of the gradient to the P-rich end and thereby also crossed the values obtained in the uniform metaecosystems. However, toward the end of the experiment, the high RUE_P in the P-poor patches 1 and 2 declined, resulting in a final unimodal pattern with lower RUE_P at both ends of the gradient compared to the uniform metaecosystems. This trend was comparable across connectivity treatments and reflected the N:P ratio of the remaining nutrients as well as P incorporation in the algae (see N:P and C:P ratios). The temporal decline of RUE_P correspondingly depended on spatial resource supply, and patch position as well as the interaction of connectivity



and spatial resource supply were significant, but based on the temporal dynamics, the main effects of both treatments were not (table 2).

Biodiversity and Dissimilarity in Species Composition (Hypothesis H3)

At the regional metaecosystem scale, ENS declined over time but was not significantly affected by treatments (fig. 3b; table 2). By contrast, final species composition was significantly more dissimilar between patches in the gradient nutrient treatment than in the uniform treatment (fig. 3c; table 2). This effect of gradients on compositional dissimilarity increased over time (significant positive temporal trend and significant interaction between time and spatial resource supply).

At the local scale, the negative temporal trend in ENS remained significant. Additionally, a significant interaction between treatments resulted from higher ENS in highly connected gradients than in highly connected uniform metaecosystems (fig. 4d; table 2). Moreover, this was amended by a significant effect of patch position (lower ENS at patch 5, the P-rich end of the gradient). Higher ENS was strongly associated with a decline in the dominance of the diatom *Ceratoneis*, which was contributing most biovolume across patches in the uniform spatial resource supply (app. D). It also dominated the low-connectivity gradient metaecosystems, especially at the P-rich end of the gradient (>80% of total biovolume, reflected by low ENS). In the highly connected gradient metaecosystems, two other species (*Teleaulax* and *Gyrosigma*) contributed larger amounts of the biovolume, especially in the N-rich patches, resulting in the higher ENS observed.

Discussion

The spatial resource supply treatment distributed the same regional amount of two essential nutrients differently among local patches, which significantly altered the uptake of the nutrients, the stoichiometry of autotroph biomass, and the transfer of available nutrients into biovolume production. These effects of spatial inequality of resource supply were more pronounced if connectivity was low, whereas in more open systems gradients were homogenized and differences to uniform metaecosystems were smaller. Concisely, we found that in gradient metaecosystems less nutrients were incorporated overall and locally in patches with highest and

Figure 3: Regional total biovolume (a), effective number of species (b), and dissimilarity in species composition between patches (c) over time. Symbols denote low (triangle) and high (circle) connectivity for uniform (gray) and gradient (black) metaecosystems. An error bar indicates standard error (\pm SE).

Table 2: Summary of the statistical analyses for response variables at regional and local scales over time

	Regional			Local			
	Biovolume	ENS	DISS	Biovolume	RUE _N	RUE _P	ENS
ME ID	6.45%	23.43%	18.10%	4.24%	2.15%	3.63%	.56%
Day	26.97%	12.59%	0%	9.72%	7.25%	9.01%	2.71%
SRS	4.01 [.083] G < U	.22	6.31 [.026] G > U	15.85 [.004] G < U	28.99 [<.001] G < U	2.71	.88
CON	7.48 [.026] L > H	1.27	.01	5.81 [.039] L > H	34.63 [<.001] L > H	1.14	3.03
SRS × CON	.27	2.35	.07	.07	19.73 [.002] G:H < all	19.91 [.002] G:H > U:H, U:H < U:L	3.69 [.091] G:H > U:H
Patch position SRS	NA	NA	NA	3.82 G: 1 < (3, 4, 5)	14.48 [<.001] G: 1 < (3, 4, 5); 2 < (3; 4, 5)	3.07 [.011] G: (1, 2, 3) > 5	3.63 [.004] G: (1, 2, 3, 4) > 5
Time (T)	10.29 [.003] -.055	32.40 [<.001] -.077	34.83 [<.001] +.014	16.60 [<.001] -.063	16.77 [<.001] -.06	16.64 [<.001] -.063	86.85 [<.001] -.07
T × CON	1.21	2.13	.36	.34	.21	.30	1.95
T × SRS	.48	.55	6.11 [.019]	5.01 [.026]	3.72 [.055]	4.62 [.033]	.47
T × CON × SRS	.08	.01	.01	.06	.04	.05	.09

Note: Fixed factors comprised the treatments' spatial resource supply (SRS) and connectivity (CON) at both scales. At the local scale, patch position (nested in SRS) was added as a fixed effect and metaccosystem ID (ME ID) was added as a random factor. Time was added as a random factor (categorically) and as a fixed factor (continuously). Response variables comprised the total biovolume, the resource use efficiency as biovolume per supplied nitrogen and phosphorus (RUE_N, RUE_P), the effective number of species (ENS), and the dissimilarity (DISS) of species composition between patches. The latter could be calculated only at the regional level, whereas RUE were analyzed only at local levels, as the regionally supplied N and P did not differ between treatments. Response variables were log transformed to achieve homogenous variances (see "Methods"). We report *F* ratios (df = 1, 8, except for the nested patch factor with df = 8, 40) as well as significance levels for all factors with *P* < .1 in brackets. We report significant differences for post hoc comparisons, abbreviating SRS levels as G (gradient) and U (uniform) and CON levels as L (low) and H (high). Boldface data indicates that *P* < .05, and italicized data indicates that .1 > *P* > .05.

lowest N:P supply (accepting H1a). Whereas the N:P ratios of remaining nutrients reflected the N:P of supply, the algal N:P and C:P changed unimodally along the gradient, as at highest N:P supply, N uptake was impaired (accepting H1b). The differences between gradient and uniform resource supply were reduced with increasing connectivity for N (remaining N and N:P ratio) but not for remaining P and algal stoichiometry (partly accepting H1c). As a consequence of less efficient nutrient uptake, gradient metaecosystems were characterized by lower overall biovolume production, especially at the scale of local patches (accepting H2). This result became even clearer when calculating local RUE standardizing biovolume by available N or P. RUE_N decreased when N supply increased, as less of the available N could be transferred into production, especially at low P and low connectivity. In a mirrorlike pattern, RUE_P decreased when P supply increased, but over time RUE_P decreased even at lowest P supply as biovolume production decreased substantially. Gradient metaecosystems showed only marginally higher effective species number and only at the local scale (partly rejecting H3), but we found the expected higher dissimilarity in species composition between patches in gradients (partly accepting H3).

*Metaecosystems, Metacommunities,
and the Role of Connectivity*

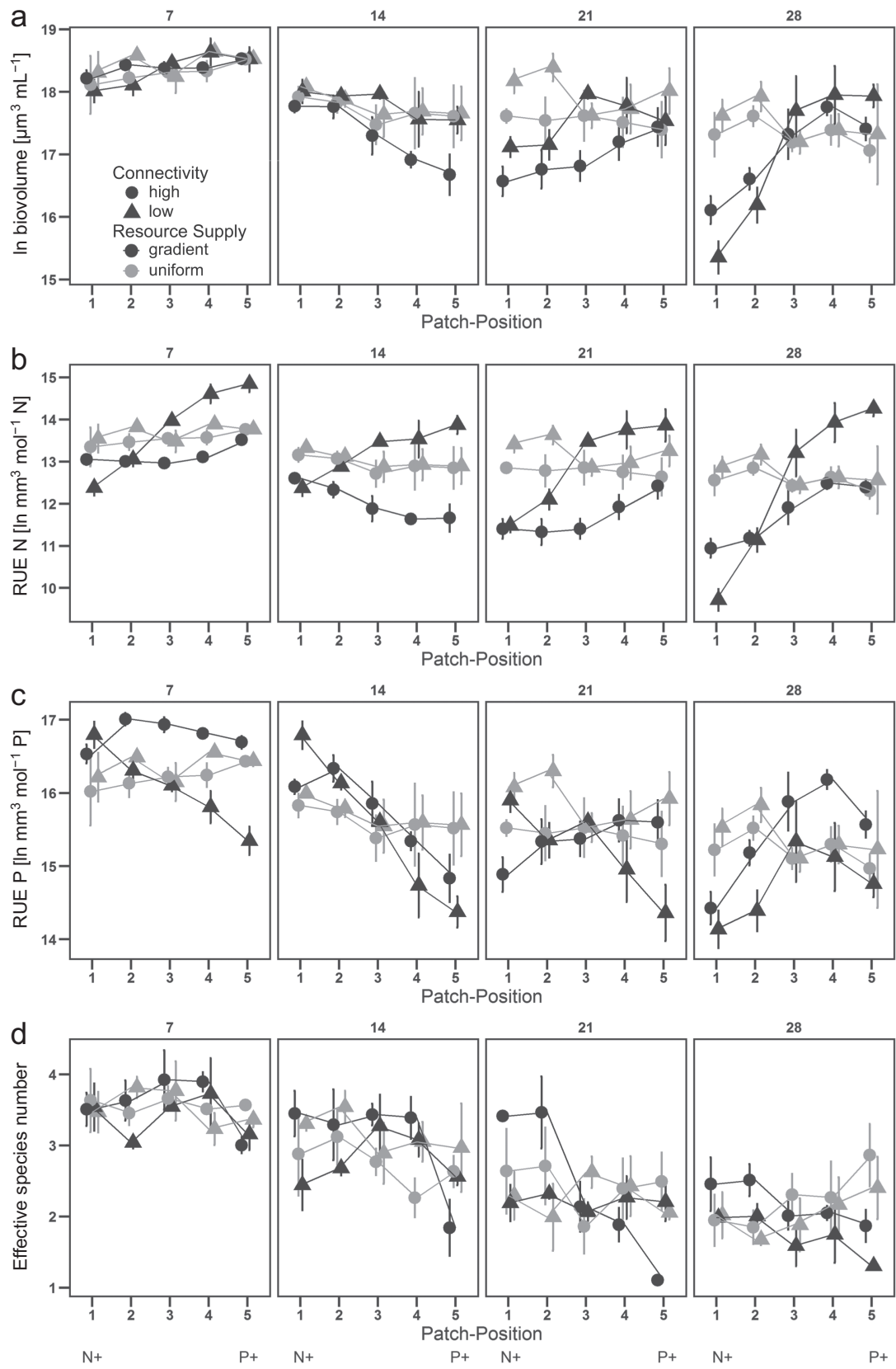
The simultaneous analysis of organism dispersal and the reciprocal flow of nutrients between patches is one of the key aspects of metaecosystem theory (Loreau et al. 2003b; Massol et al. 2011) and the few experiments conducted in this field (Staddon et al. 2010; Legrand et al. 2012; Harvey et al. 2016; Limberger et al. 2017). Often, metaecosystem models are explicitly built to separately assess the different flows of matter induced by organism dispersal and abiotic resource diffusion (Gounand et al. 2018), and this has been included in some of the existing experiments (Limberger et al. 2017). Instead, our experiment focused on two different levels of connectivity, as one important, straightforward conclusion from metaecosystem theory is that higher connectivity dampens the effect of environmental heterogeneity between patches (Gounand et al. 2014). In designing the experiment, we opted for dispersal involving active movement, whereas any treatment manipulating organisms independent of abiotic nutrient flow would require pipetting as the transfer method, which eliminates differences in dispersal abilities. Thus, our setup addressed the effect of connectivity on simultaneous particulate and dissolved matter fluxes in metaecosystems of different connectivity and environmental heterogeneity.

The interdependence of connectivity and spatial resource supply was reflected by many significant interaction terms in

the statistical analyses. However, these interactions were not consistent across response variables: regionally, they were significant for remaining N concentrations and N:P ratios but not for remaining P, resulting in the highest amount of unutilized N in less connected gradient metaecosystems. At the local scale, the significant effect of patch position on remaining nutrients, algal stoichiometry, and RUE were all tested (and significant) across connectivity levels but were often much more pronounced at low connectivity. Thus, the difference between gradient and uniform metaecosystems became smaller if high connectivity homogenized nutrients over time (high connectivity) but with different consequences for the spatial dynamics of N and P. A potential reason for this difference is faster local uptake of P than N and thus P being depleted before connectivity effects can emerge.

Metacommunity models also predict that connectivity and spatial resource supply jointly affect species composition, as species sorting causes higher dissimilarity in species composition with increasing heterogeneity in environmental conditions under low connectivity (Cottenie 2005). In line with these predictions, we found higher compositional dissimilarity between patches in gradient than in uniform metaecosystems, a difference that additionally intensified over time. However, connectivity did not affect this difference significantly, which shows that high connectivity levels were not high enough to promote regional dominance through source-sink dynamics and mass effects (Mouquet and Loreau 2003). Such regional dominance would reduce dissimilarity in species composition between patches under high connectivity, as has been shown in some empirical studies using rock pool communities (Vanschoenwinkel et al. 2007), plankton communities (Limberger et al. 2017), or benthic microalgae (Matthiessen et al. 2010).

In our study, a single species, *Ceratoneis*, dominated all local assemblages in the uniform metaecosystems and the low-connectivity gradients, whereas two additional species needed higher opening times and the spatial heterogeneity of the gradients to dominate over *Ceratoneis*. This resulted in the higher ENS in the highly connected gradient metaecosystems and superficially supports the idea that higher immigration reduces local dominance (Loreau and Mouquet 1999). However, the picture is complicated somewhat by the fact that—at low connectivity—*Ceratoneis* dominated the entire range of local patches from highest to lowest N:P. *Ceratoneis* is characterized by high potential growth rate and multiple movement modes (Apoya-Horton et al. 2006; Kingston 2009), which might allow this species to preempt nutrient uptake (through fast reproduction) and transfer between patches efficiently, even under low connectivity. This advantage might be reduced under high connectivity, allowing other species to transfer efficiently through the silicon tubes as well. In the lack of direct observation of motility, we cannot



fully resolve this picture, but it aligns with the higher local ENS that we found in well-connected gradients.

Stoichiometry of Resource Supply and Resource Use in Metaecosystems

Few models have explicitly analyzed how spatial heterogeneity in the stoichiometry of resource supply alters resource uptake and transfer into biomass production in spatially connected systems (Codeco and Grover 2001; Gross and Cardinale 2007; Marleau et al. 2015; Hodapp et al. 2016; Leroux et al. 2017). Whereas our experiment differs from any of these models in at least one central aspect, our empirical observations are remarkably well in line with the main predictions derived from these models. The gradostat approach modeled (and empirically tested) by Codeco and Grover (2001) and the metacommunity model by Gross and Cardinale (2007) included two countercurrent resource gradients and found lower efficiency in transferring resources to biomass in the stoichiometrically most extreme patches. Gross and Cardinale (2007) also predicted higher overall biomass at the intermediate patch position, which in the case of our experiment was observed only if we standardized biovolume by P supply, revealing a unimodal pattern of RUE_p across the gradient metaecosystems. Hodapp et al. (2016) constructed a two-dimensional model allowing for organism dispersal but no nutrient diffusion as in our experiment. Still, as in their model, we found higher remaining nutrient concentrations and lower biovolume production in the gradient metaecosystems (analogous to the environmentally more heterogeneous scenarios in the model) at regional and local scales.

RUE for N and P declined in the patches with the highest and lowest N:P supply ratios, respectively. This low RUE was partly based on the inefficiency to access available resources if one resource, in this case P, was in very low supply. As supplied N:P ratios increased from patch 5 to patch 1 in our gradient metaecosystems, algal N:P and C:P also increased for most of this gradient. However, we found a remarkable deviation from the very low P supply at patch 1 in the low-connectivity treatment, as N:P and C:P decreased again and were significantly lower than in patch 2 (and 3 for C:P). Reflecting the results for algal C:P ratio in the gradient metaecosystems, RUE_p also changed from a linear decline with patch position after 2 weeks (reflecting the surplus of P) to a unimodal pattern with low RUE_p in patch 1 after 4 weeks. Thus, the lack of P resulted in low N incorporation, C fixation, and biovolume production at this gradient position, which strongly points toward “biochemical colimita-

tion.” This inability to use an available resource because a second resource is missing has been identified as one pathway for multiple resource limitation (Danger et al. 2008; Saito et al. 2008; Harpole et al. 2011). Generally, phytoplankton elemental composition reflects the availability of nutrients in the field (Guildford and Hecky 2000) and in experiments (Hillebrand et al. 2013). A closer inspection of the field data used by Guildford and Hecky (2000), however, shows a similar deviation of incorporation from supply at extreme supply ratios: at highest total N:total P ratios (proxy of supply), both algal N:P and C:P decreased. It thus seems that the stoichiometric consequences of imbalanced supply observed in our microcosm metaecosystems can be observed in field situations as well.

Extending beyond our experiment with a single trophic level, such colimitation patterns can also emerge at the regional scale if resources, autotrophs, and herbivores have different mobility rates (Marleau et al. 2015). Leroux et al. (2017) extended this idea toward a stoichiometric distribution model to analyze how spatial patterns in plant stoichiometry alter the space use of a mobile herbivore. Despite the conceptual differences between these models and our experiment, they highlight two important aspects in our study. First, different mobility of organisms affects spatial resource flow, and it will strongly alter the relative importance of resource flow via organism dispersal compared to the flow of available resources via diffusion or water transport. Whereas we have a relatively good estimation of the latter based on our additional experiment (app. B), the former could not be quantified, as we opted for direct connectivity rather than transfer through pipetting (see above). However, we assume that the latter is less important than the supply of dissolved nutrients, given the clear gradient in remaining dissolved N:P over patch position in the low-connectivity gradients. Second, the stoichiometric distribution model (Leroux et al. 2017) allows a strong link to biogeochemistry at the spatial scales relevant to element cycles, as a mobile consumer, for example, might induce stoichiometrically explicit resource flows if feeding and excretion occur in different patches (McIntyre et al. 2008).

Consequences for Cross-System Subsidies

Many ecosystems are characterized by reciprocal subsidies from adjacent habitat types, which include organism dispersal (e.g., insects emerging from streams and entering terrestrial food webs) and abiotic matter flow (e.g., dissolved or particulate matter from terrestrial systems into streams; Baxter et al. 2004; Gratton and Vander Zanden 2009; Dreyer

Figure 4: Local total biovolume (*a*), resource use efficiency (RUE) for nitrogen (N; *b*) and phosphorus (P; *c*), and effective species number (*d*) over time (panels from left to right: day 7, 14, 21, and 28) and patch position (1–5) in metaecosystems differing in spatial resource supply (gradient: black; uniform: gray) at low (triangle) and high (circle) connectivity. An error bar indicates standard error ($\pm SE$).

et al. 2015). Given that these subsidies often comprise differentiated anorganic and dispersal-dependent matter flows, the analysis of these cross-system linkages strongly profits from a metaecosystem perspective (Leroux and Loreau 2008, 2012; Gounand et al. 2017, 2018). In addition to addressing the relative role of different agents of connectivity (organisms, detritus, anorganic matter flow), a stoichiometric perspective will be useful as the material exchanged between systems will differ in not only quantity but also quality (Sitters et al. 2015; Soininen et al. 2015).

A recent meta-analysis (Bartels et al. 2012) shows that terrestrial systems receive less allochthonous material than freshwater systems but often in the form of nutrient-rich organisms channeled as high-quality prey for predator levels. Freshwater systems receive more material but mainly in the form of carbon-rich, nutrient-poor dead organic matter channeled into the detritus pathway. Here an explicit metaecosystem approach can be a useful tool to understand cross-system dynamics merging food web dynamics, stoichiometry of allochthonous material, and the relative role of matter flow and organism dispersal (Leroux and Loreau 2012; Gounand et al. 2018).

Additional future avenues extending the results from our study would be an explicit assessment of organismic nutrient transport, preferentially in a multitrophic context, as well as altered spatial network structures. Our experiment comprised a single (and simple) geometric arrangement of patches in the form of a linear chain. Whereas this enabled testing the specific hypotheses of our article, we would like to stress the important conclusion from models and empirical analyses that emergent properties of spatial networks are strongly affected by the concise spatial structure of the network (Marleau et al. 2014). For example, this has been clearly shown by work on dendritic networks as found in river systems, where topology plays a central role in defining regional dynamics (Carrara et al. 2012; Altermatt and Fronhofer 2018). Actually, most realized metaecosystems have a finite spatial structure that differs from the limiting cases often used to address spatial dynamics in models (Marleau et al. 2014). Thus, an important question posed to future metaecosystem approaches will be to generate conclusions beyond the specific spatial arrangement of connectivity.

Acknowledgments

This article benefited greatly from fruitful comments by Spencer Hall, two anonymous reviewers, Robert Ptacnik, Alexey Ryabov, Maren Striebel, and Nina Welti. Silke Ammermann and Heike Rickels are gratefully acknowledged for help in the laboratory. This study was financially supported by funding from the German Research Foundation to H.H. (contract Hi 848/8-1).

Statement of authorship: N.G. and H.H. designed the experiment; N.G. and Y.W. conducted the experiment and analyzed samples; N.G. and H.H. analyzed the data; and N.G. and H.H. wrote the manuscript.

Literature Cited

- Altermatt, F., and E. A. Fronhofer. 2018. Dispersal in dendritic networks: ecological consequences on the spatial distribution of population densities. *Freshwater Biology* 63:22–32.
- Apoya-Horton, M. D., L. Yin, G. J. C. Underwood, and M. R. Gretz. 2006. Movement modalities and responses to environmental changes of the mudflat diatom *Cylindrotheca closterium* (Bacillariophyceae). *Journal of Phycology* 42:379–390.
- Bartels, P., J. Cucherousset, K. Steger, P. Eklov, L. J. Tranvik, and H. Hillebrand. 2012. Reciprocal subsidies between freshwater and terrestrial ecosystems structure consumer resource dynamics. *Ecology* 93:1173–1182.
- Bates, D., M. Mächler, B. Bolker, and S. Walker. 2015. Fitting linear mixed-effects models using lme4. *Journal of Statistical Software* 67:48.
- Baxter, C. V., K. D. Fausch, M. Murakami, and P. L. Chapman. 2004. Fish invasion restructures stream and forest food webs by interrupting reciprocal prey subsidies. *Ecology* 85:2656–2663.
- Bray, J. R., and J. T. Curtis. 1957. An ordination of the upland forest communities of southern Wisconsin. *Ecological Monographs* 27:325–349.
- Carrara, F., F. Altermatt, I. Rodriguez-Iturbe, and A. Rinaldo. 2012. Dendritic connectivity controls biodiversity patterns in experimental metacommunities. *Proceedings of the National Academy of Sciences of the USA* 109:5761–5766.
- Chase, J. M., and T. M. Knight. 2013. Scale-dependent effect sizes of ecological drivers on biodiversity: why standardised sampling is not enough. *Ecology Letters* 16:17–26.
- Codeco, C. T., and J. P. Grover. 2001. Competition along a spatial gradient of resource supply: a microbial experimental model. *American Naturalist* 157:300–315.
- Cottenie, K. 2005. Integrating environmental and spatial processes in ecological community dynamics. *Ecology Letters* 8:1175–1182.
- Danger, M., T. Daufresne, F. Lucas, S. Pissard, and G. Lacroix. 2008. Does Liebig's law of the minimum scale up from species to communities? *Oikos* 117:1741–1751.
- Dreyer, J., P. A. Townsend, J. C. Hook III, D. Hoekman, M. J. Vander Zanden, and C. Gratton. 2015. Quantifying aquatic insect deposition from lake to land. *Ecology* 96:499–509.
- Elton, C. S. 1958. *The ecology of invasions by animals and plants*. Methuen, London.
- Gounand, I., E. Harvey, P. Ganesanandamoorthy, and F. Altermatt. 2017. Subsidies mediate interactions between communities across space. *Oikos* 126:972–979.
- Gounand, I., E. Harvey, C. J. Little, and F. Altermatt. 2018. Metaecosystems 2.0: rooting the theory into the field. *Trends in Ecology and Evolution* 33:36–46.
- Gounand, I., N. Mouquet, E. Canard, F. Guichard, C. Hauzy, and D. Gravel. 2014. The paradox of enrichment in metaecosystems. *American Naturalist* 184:752–763.
- Grasshoff, K., M. Ehrhardt, and K. Kremling. 1983. *Methods of seawater analysis*. 2nd ed. Chemie, Weinheim.

- Gratton, C., and M. J. Vander Zanden. 2009. Flux of aquatic insect productivity to land: comparison of lentic and lotic ecosystems. *Ecology* 90:2689–2699.
- Gravel, D., F. Guichard, M. Loreau, and N. Mouquet. 2010a. Source and sink dynamics in meta-ecosystems. *Ecology* 91:2172–2184.
- Gravel, D., N. Mouquet, M. Loreau, and F. Guichard. 2010b. Patch dynamics, persistence, and species coexistence in metaecosystems. *American Naturalist* 176:289–302.
- Gross, K., and B. J. Cardinale. 2007. Does species richness drive community production or vice versa? reconciling historical and contemporary paradigms in competitive communities. *American Naturalist* 170:207–220.
- Grunwald, M., O. Dellwig, G. Liebezeit, B. Schnetger, R. Reuter, and H. J. Brumsack. 2007. A novel time-series station in the Wadden Sea (NW Germany): first results on continuous nutrient and methane measurements. *Marine Chemistry* 107:411–421.
- Guildford, S. J., and R. E. Hecky. 2000. Total nitrogen, total phosphorus, and nutrient limitation in lakes and oceans: is there a common relationship? *Limnology and Oceanography* 45:1213–1223.
- Guillard, R. R. L., and J. H. Ryther. 1962. Studies on marine planktonic diatoms. I. *Cyclotella nana* Husted, and *Detonula confervaceae* (Cleve) Gran. *Canadian Journal of Microbiology* 8:229–239.
- Gülzow, N., Y. Wahlen, and H. Hillebrand. 2018. Data from: Meta-ecosystem dynamics of marine phytoplankton alters resource use efficiency along stoichiometric gradients. *American Naturalist*, Dryad Digital Repository, <https://dx.doi.org/10.5061/dryad.km10jq1>.
- Haegeman, B., and M. Loreau. 2014. General relationships between consumer dispersal, resource dispersal and metacommunity diversity. *Ecology Letters* 17:175–184.
- Harpole, W. S., J. T. Ngai, E. E. Cleland, E. W. Seabloom, E. T. Borer, M. E. S. Bracken, J. J. Elser, et al. 2011. Nutrient co-limitation of primary producer communities. *Ecology Letters* 14:852–862.
- Harvey, E., I. Gounand, P. Ganesanandamoorthy, and F. Altermatt. 2016. Spatially cascading effect of perturbations in experimental meta-ecosystems. *Proceedings of the Royal Society B* 283:20161496.
- Hillebrand, H., C. D. Duerksen, D. B. Kirschtel, U. Pollinger, and T. Zohary. 1999. Biovolume calculation for pelagic and benthic microalgae. *Journal of Phycology* 35:403–424.
- Hillebrand, H., G. Steinert, M. Boersma, A. M. Malzahn, C. L. Meunier, C. Plum, and R. Ptacnik. 2013. Goldman revisited: faster growing phytoplankton has lower N:P and lower stoichiometric flexibility. *Limnology and Oceanography* 58:2076–2088.
- Hodapp, D., H. Hillebrand, B. Blasius, and A. B. Ryabov. 2016. Environmental and trait variability constrain community structure and the biodiversity-productivity relationship. *Ecology* 97:1463–1474.
- Holyoak, M., M. A. Leibold, N. M. Mouquet, R. D. Holt, and M. F. Hoopes. 2005. Metacommunities: a framework for large-scale community ecology. Pages 1–31 in M. Holyoak, M. A. Leibold, and R. D. Holt, eds. *Metacommunities—spatial dynamics and ecological communities*. University of Chicago Press, Chicago.
- Kingston, M. B. 2009. Growth and motility of the diatom *Cylindrotheca closterium*: implications for commercial applications. *Journal of the North Carolina Academy of Science* 125:138–142.
- Legrand, D., O. Guillaume, M. Baguette, J. Cote, A. Trochet, O. Calvez, S. Zajitschek, et al. 2012. The Metatron: an experimental system to study dispersal and metaecosystems for terrestrial organisms. *Nature Methods* 9:828–833.
- Leibold, M. A., J. M. Chase, and S. K. M. Ernest. 2017. Community assembly and the functioning of ecosystems: how metacommunity processes alter ecosystems attributes. *Ecology* 98:909–919.
- Leibold, M. A., M. Holyoak, N. Mouquet, P. Amarasekare, J. M. Chase, M. F. Hoopes, R. D. Holt, et al. 2004. The metacommunity concept: a framework for multi-scale community ecology. *Ecology Letters* 7:601–613.
- Leibold, M. A., and G. M. Mikkelsen. 2002. Coherence, species turnover, and boundary clumping: elements of meta-community structure. *Oikos* 97:237–250.
- Lenth, R. V. 2016. Least-squares means: the R package lsmeans. *Journal of Statistical Software* 69:1–33.
- Leroux, S. J., and M. Loreau. 2008. Subsidy hypothesis and strength of trophic cascades across ecosystems. *Ecology Letters* 11:1147–1156.
- . 2012. Dynamics of reciprocal pulsed subsidies in local and meta-ecosystems. *Ecosystems* 15:48–59.
- Leroux, S. J., E. V. Wal, Y. F. Wiersma, L. Charron, J. D. Ebel, N. M. Ellis, C. Hart, et al. 2017. Stoichiometric distribution models: ecological stoichiometry at the landscape extent. *Ecology Letters* 20:1495–1506.
- Limberger, R., J. Birtel, D. d. S. Farias, and B. Matthews. 2017. Ecosystem flux and biotic modification as drivers of metaecosystem dynamics. *Ecology* 98:1082–1092.
- Logue, J. B., N. Mouquet, H. Peter, H. Hillebrand, and Metacommunity Working Group. 2011. Empirical approaches to metacommunities: a review and comparison with theory. *Trends in Ecology and Evolution* 26:482–491.
- Loreau, M., and R. D. Holt. 2004. Spatial flows and the regulation of ecosystems. *American Naturalist* 163:606–615.
- Loreau, M., and N. Mouquet. 1999. Immigration and the maintenance of local species diversity. *American Naturalist* 154:427–440.
- Loreau, M., N. Mouquet, and A. Gonzalez. 2003a. Biodiversity as spatial insurance in heterogeneous landscapes. *Proceedings of the National Academy of Sciences of the USA* 100:12765–12770.
- Loreau, M., N. Mouquet, and R. D. Holt. 2003b. Meta-ecosystems: a theoretical framework for a spatial ecosystem ecology. *Ecology Letters* 6:673–679.
- Marleau, J. N., F. Guichard, and M. Loreau. 2014. Meta-ecosystem dynamics and functioning on finite spatial networks. *Proceedings of the Royal Society B* 281:20132094.
- . 2015. Emergence of nutrient co-limitation through movement in stoichiometric meta-ecosystems. *Ecology Letters* 18:1163–1173.
- Massol, F., D. Gravel, N. Mouquet, M. W. Cadotte, T. Fukami, and M. A. Leibold. 2011. Linking community and ecosystem dynamics through spatial ecology. *Ecology Letters* 14:313–323.
- Matthiessen, B., E. Mielke, and U. Sommer. 2010. Dispersal decreases diversity in heterogeneous metacommunities by enhancing regional competition. *Ecology* 91:2022–2033.
- McIntyre, P. B., A. S. Flecker, M. J. Vanni, J. M. Hood, B. W. Taylor, and S. A. Thomas. 2008. Fish distributions and nutrient cycling in streams: can fish create biogeochemical hotspots? *Ecology* 89:2335–2346.
- Mouquet, N., and M. Loreau. 2003. Community patterns in source-sink metacommunities. *American Naturalist* 162:544–557.
- Oksanen, J., F. G. Blanchet, R. Kindt, P. Legendre, P. R. Minchin, R. B. O'Hara, G. L. Simpson, et al. 2015. *vegan*: community ecology package. R package version 2.2-1. <https://CRAN.R-project.org/package=vegan>.
- Olenina, I., S. Hajdu, L. Edler, A. Andersson, N. Wasmund, S. Busch, J. Göbel, et al. 2006. Biovolumes and size-classes of phytoplankton in the Baltic Sea. *Baltic Sea Environment Proceedings*. Vol. 106. Baltic Marine Environment Protection Commission, Helsinki.

- R Development Core Team. 2015. R: a language and environment for statistical computing. R Foundation for Statistical Computing, Vienna.
- Saito, M. A., T. J. Goepfert, and J. T. Ritt. 2008. Some thoughts on the concept of colimitation: three definitions and the importance of bioavailability. *Limnology and Oceanography* 53:276–290.
- Sitters, J., C. L. Atkinson, N. Guelzow, P. Kelly, and L. L. Sullivan. 2015. Spatial stoichiometry: cross-ecosystem material flows and their impact on recipient ecosystems and organisms. *Oikos* 124:920–930.
- Soininen, J., P. Bartels, J. Heino, M. Luoto, and H. Hillebrand. 2015. Toward more integrated ecosystem research in aquatic and terrestrial environments. *Bioscience* 65:174–182.
- Staddon, P., Z. Lindo, P. D. Crittenden, F. Gilbert, and A. Gonzalez. 2010. Connectivity, non-random extinction and ecosystem function in experimental metacommunities. *Ecology Letters* 13:543–552.
- Turner, M. G. 1989. Landscape ecology: the effect of pattern on process. *Annual Review of Ecology and Systematics* 20:171–197.
- . 2005. Landscape ecology: what is the state of the science? *Annual Review of Ecology Evolution and Systematics* 36:319–344.
- Vanschoenwinkel, B., C. De Vries, M. Seaman, and L. Brendonck. 2007. The role of metacommunity processes in shaping invertebrate rock pool communities along a dispersal gradient. *Oikos* 116:1255–1266.
- Wickham, H. 2009. *ggplot2—elegant graphics for data analysis*. Use R! Series. Springer, New York.

Associate Editor: Spencer R. Hall
Editor: Judith L. Bronstein



Experimental setup for the metaecosystem experiment. Photo credit: Yanis Wahlen.